Annals of Operations Research (2026) 361:1447–1471
https://doi.org/10.1007/s10479-024-06426-2

ORIGINAL RESEARCH

Resilience analysis based on multi-layer network community detection of supply chain network

Yingqiu Zhu[1] · Yilin Bao[1] · Lei Qin[1,2] · Qiang Sun[1] · Ben-Chang Shia[3,4] · Ming-Chih Chen[3,4]

Received: 29 June 2024 / Accepted: 27 November 2024 / Published online: 7 January 2025
© The Author(s) 2025

Abstract
As the economic environment becomes increasingly complex, enhancing supply chain resilience is crucial for the operations and long-term development of enterprises. Real-world supply chains, encompassing components such as goods, warehouses, and plants, often contain complex network structures, making resilience analysis a challenging task. This paper addresses this challenge from a network analysis perspective. We project the complex supply chain network into single-mode, multi-layer networks focusing on plants and warehouses. Utilizing a multi-layer community detection method, we identify local clusters within these networks. By uncovering closely connected clusters, we reveal the flexibility and redundancy in production capabilities among different plants and warehouses. An empirical study using real-world data demonstrates that multi-layer network clustering effectively uncovers indirect capacity linkages between plants and warehouses. The findings from this community detection are beneficial for strategic capacity management, aiding enterprises in managing supply shortages or sudden demand spikes.

Keywords Resilience analysis · Supply chain · Community detection

✉ Ming-Chih Chen
081438@mail.fju.edu.tw

Yingqiu Zhu
inqzhu@uibe.edu.cn

Yilin Bao
b1071280971@163.com

Lei Qin
qinlei@uibe.edu.cn

Qiang Sun
sunqiang@uibe.edu.cn

Ben-Chang Shia
025674@mail.fju.edu.tw

1 School of Statistics, University of International Business and Economics, Beijing, China

2 Dong Fureng Institute of Economic and Social Development, Wuhan University, Wuhan, China

3 Graduate Institute of Business Administration, College of Management, Fu Jen Catholic University, New Taipei City, Taiwan

4 Artificial Intelligence Development Center, Fu Jen Catholic University, New Taipei City, Taiwan

1 Introduction

In today's increasingly complex socio-economic environment, enterprises' supply chains face mounting threats, including catastrophic earthquakes, political instability, fuel shortages, disease outbreaks, and acts of terrorism (Sodhi et al., 2012; Chen et al., 2013; Ho et al., 2015; Son et al., 2021). A supply chain is a network of facilities that deliver plants or services from producers to consumers (Ellram et al., 2004). Typically, real-world supply chains manifest as complex logistics systems involving plants, warehouses, and distribution channels. For enterprises, effective supply chain management aims to handle the flow of goods efficiently and sustainably (Mentzer et al., 2001). As the economic environment grows more volatile, the likelihood of external shocks impacting supply chains also increases. Unforeseen "black swan" events, such as the COVID-19 pandemic, can have devastating effects on supply chains. When nodes or channels within the supply chain are incapacitated, the efficiency of the entire production and transportation process can be compromised, leading to significant economic losses for enterprises, including declines in operating income, return on sales, return on assets and stock market valuation (Hendricks & Singhal, 2003). Given the potentially sever impact of supply chain disruptions, enhancing supply chain resilience, defined as the capacity to persist, adapt, or transform in the face of change (Wieland & Durach, 2021), is imperative.

The significance of supply chain resilience analysis has been increasingly recognized. Mandal (2012) have associated resilience with the capability to rapidly restore supply chains to normal operations or enhance operational efficiency following disruptive events. Tukamuhabwa et al. (2015) have emphasized that a company's ability to respond more effectively to disturbances compared to its competitors can strengthen its market position. Consequently, fostering a resilient supply chain is advantageous for both short-term survival and long-term competitiveness. Gao et al. (2016) have advocated resilience as a crucial solution for supply chains to navigate turbulent scenarios. Scholars have also proposed extending organizational risk management practices to the realm of supply chains (Fan & Stevenson, 2018; Norrman & Wieland, 2020). From a risk management perspective, the aim of resilience analysis lies in identifying, assessing, controlling, and monitoring various sources of risk that could disrupt supply chains. However, a supply chain comprises a complex network of interconnected organizations, transcending the sum of its parts and exhibiting dynamic characteristics. Hence, there are fundamental disparities between organizational risk management and the analysis of supply chain resilience. Davoudi et al. (2013) have argued that resilience analysis should concentrate on the systemic attributes of supply chains rather than individual risk sources. To systematically evaluate the resilience of a supply chain, this paper explores the network structure within the chain and studies its characteristics through network analysis.

From a network perspective, a crucial mechanism for enhancing the resilience of a supply chain is the augmentation of redundancy. By incorporating redundant nodes, such as duplicate manufacturing plants or surplus inventory within the supply chain, enterprises can effectively navigate supply shortages or sudden spikes in demand through strategic allocation of surplus resources (Maharjan & Kato, 2022). Maintaining spare capacity along critical pathways within the supply chain is essential for cultivating resilience (Pavlov et al., 2019). The duplication of capacity enables enterprises to implement contingency measures to uphold operations during instances of managerial failure. Moreover, redundancy is expected to increase the flexibility of the supply chain, allowing enterprises to expedite resource deployment or preempt delays (Jüttner et al., 2003; Johnson et al., 2013; Kristianto et al., 2014). However, increasing redundancy in a supply chain remains a challenging problem. Enterprise managers face several critical questions, such as which parts of the supply

chain need duplication and where capacity expansion is required. To provide decision-making support for these concerns, we propose integrating community detection methods, widely utilized for uncovering network structures, to enhance the analysis of supply chain resilience. Our objective is to detect communities within a supply chain (e.g., groups comprise closely interconnected plants and warehouses) and partition the supply chain into several densely connected communities. We then study strategies for augmenting redundancy by investigating the node distributions within each community and identifying crucial nodes that bridge different communities.

In multi-layer networks of complex systems like supply chains, community detection presents unique challenges compared to single-layer networks (Huang et al., 2021). The primary objective is to uncover a shared community structure across multiple layers, identifying groups of well-connected nodes. Various community detection methods originally developed for single-layer networks have been adapted to accommodate the complexities of multi-layer networks. For instance, the modularity metric, which evaluates the quality of divisions in a single-layer network, has been extended to multi-layer modularity density, resulting in modularity-based community detection methods for multi-layer networks (Ma et al., 2018). Tagarelli et al. (2017) have proposed an ensemble-based approach to aggregate community structures detected independently in each layer to form a comprehensive partition of all nodes. Additionally, spectral clustering methods have been extended to multi-layer versions to ensure consistent community detection in multi-layer networks (Lei et al., 2019). Further research on this topic is available in (Kim & Lee, 2015; Huang et al., 2021; Ma & Nandy, 2023).

In this paper, we propose a comprehensive framework for analyzing the resilience of a supply chain through community detection in multi-layer networks. We begin by modeling the supply chain, which comprises various types of nodes, as a multi-mode network. To explore the inherent community structures, we analyze different types of nodes separately, projecting the multi-mode network into various multi-layer configurations, such as a multi-layer network of plants. By applying community detection techniques to these multi-layer networks, we can identify and understand critical local structures. This enables more effective planning and management strategies to mitigate potential risks within the supply chain. The aggregated analysis of multi-layer networks reveals global structures that may not be apparent when examining individual layers separately. Identifying common structures across different layers allows for more accurate inference results. For local communities, we examine the distributions and diversities of each type of node, assessing the redundancy and flexibility of different parts of the supply chain. The proposed framework is applicable for general supply chains. In regard to multiple relations among different objects within a supply chain, we use a multi-layer network structure to model them and thus apply the proposed community detection method. This framework aids enterprises in comprehensively considering the significance of various types of nodes in supply chain design and management. Ultimately, it enhances the resilience and risk mitigation capabilities of the supply chain.

2 Methodology

2.1 Multi-mode network of supply chain

To accurately model the network structure of a supply chain comprising various types of nodes, we define a multi-mode network $\mathcal{G} = G(E, V)$, where $V = \{V_{\mathrm{P}}, V_{\mathrm{W}}, V_{\mathrm{G}}\}$ represents

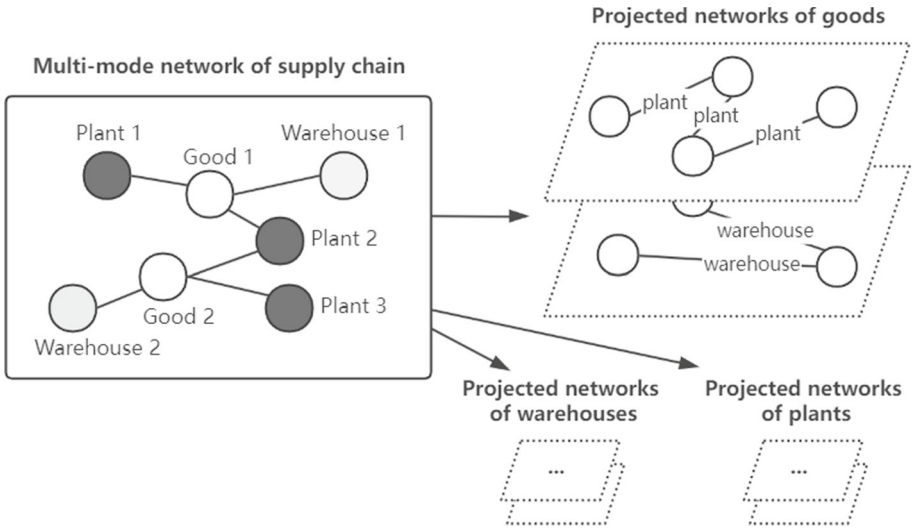

Fig. 1 Multi-mode network of supply chain (left) and projected versions of single-mode networks (right)

the set of all nodes, with V_{P}, V_{W}, and V_{G} denoting the node sets of N_{P} plants, N_{W} warehouses, and N_{G} goods, respectively. The set $E = \{(v_i, v_j) : v_i, v_j \in V_{\mathrm{P}} \cup V_{\mathrm{W}} \cup V_{\mathrm{G}}\}$ represents the set of all edges. As a representation of the supply chain, $\mathcal{G}$ effectively captures the production and distribution dynamics of the supply chain, with goods nodes playing pivotal roles. Figure 1 illustrates the structure of $\mathcal{G}$. Based on the this multi-mode network, we can derive single-mode networks through projection. For instance, a single-mode network for goods can be generated, where edges exist between any two goods if they can be produced by the same plant or stored in the same warehouse. In order to make the symbols easy to follow, we provide a summary in Table 1.[1]

It is essential to note that $\mathcal{G}$ is a comprehensive network encompassing various relationships among different types of nodes. For $v_i \in V_{\mathrm{G}}$ and $v_j \in V_{\mathrm{P}}$, an edge (v_i, v_j) indicates that the plant v_j produces the good v_i. Similarly, for $v_k \in V_{\mathrm{W}}$ and $v_i \in V_{\mathrm{G}}$, the corresponding edge signifies that the good v_i can be stored in the warehouse v_k. Direct relationships between nodes of the same type may not always exist. For instance, two plants v_{j_1} and $v_{j_2} \in V_{\mathrm{P}}$ may not have a direct relation (e.g., business cooperation), meaning $(v_{j_1}, v_{j_2}) \notin E$. However, if plants v_{j_1} and v_{j_2} produce the same plants, they can be implicitly related. If plant v_{j_1} faces operational challenges, plant v_{j_2} can sustain production, thus mitigating supply chain disruptions. In such cases, increasing the capacity of v_{j_2} may be considered by the supply chain manager to restore operational efficiency.

2.2 Projected multi-layer network

To explore implicit relations and enhance the redundancy of the supply chain, this paper leverages the indirect relations among nodes of the same type. By utilizing these indirect connections, we project the network $\mathcal{G}$ into various configurations, such as single-mode

[1] In Table 1, we take networks of goods as examples to show symbols related to single-mode networks. We use superscript (G) to denote symbols related to good nodes. For nodes of warehouses and plants, we use superscripts (W) and (P), respectively.

Table 1 Important symbols and corresponding descriptions

Symbol	Description
K	The number of communities
$\mathcal{G} = G(E, V)$	A multi-mode network with a node set V and an edge set E
N_{G}	The number of good nodes
V_{G}	Node set of N_{G} goods
v_i	The i-th individual node
$\mathcal{A}^{(\mathrm{G})}$	The projected 2-layer network of goods
$A_{\mathrm{P}}^{(\mathrm{G})}$	The adjacency matrix of the projected network of goods according to plants
$A_{\mathrm{P},ij}^{(\mathrm{G})}$	The plant-based relation between the i-th good and the j-th good
$A_{\mathrm{W}}^{(\mathrm{G})}$	The adjacency matrix of the projected network of goods according to warehouses
$A_{\mathrm{W},ij}^{(\mathrm{G})}$	The warehouse-based relation between the i-th good and the j-th good
$\Psi_k^{(\mathrm{G})}$	The index set of the k-th latent community of goods
$\psi^{(\mathrm{G})}$	The membership vector of goods
$\psi_i^{(\mathrm{G})}$	The community label of the i-th good
$\hat{\psi}^{(\mathrm{G})}$	The estimation of the membership vector of goods
B_{P}	The block matrix of community-wise edge probabilities for $A_{\mathrm{P}}^{(\mathrm{G})}$
B_{W}	The block matrix of community-wise edge probabilities for $A_{\mathrm{W}}^{(\mathrm{G})}$
$\mathcal{S}_k(\psi)$	The cardinal of the k-th community given ψ
$\Phi_k^{(\mathrm{G})}(\psi)$	The binary membership vector given ψ
$\Phi_{k,i}^{(\mathrm{G})}(\psi)$	The indicator wether $\psi_i = k$
$\widetilde{\Phi}_k^{(\mathrm{G})}(\psi)$	The normalized version of $\Phi_k^{(\mathrm{G})}(\psi)$ according to the cardinal

network of goods or two-mode network of plants and warehouses. This approach enables us to identify community structures within the supply chain by analyzing these projected single-mode networks.

The projected networks may consist of multiple layers. As the network $\mathcal{G}$ encompasses three types of nodes, the indirect relations between two nodes of the same type can be quite diverse. Consider the projected network of goods as an example. For any two goods $v_{i_1}, v_{i_2} \in V_{\mathrm{G}}$, they are considered indirectly related if they can be produced by the same plants or stored in the same warehouses. Therefore, we represent the projected network of goods using a 2-layer network with a set of adjacency matrices $\mathcal{A}^{(\mathrm{G})} = \{A_{\mathrm{P}}^{(\mathrm{G})}, A_{\mathrm{W}}^{(\mathrm{G})}\}$. These matrices delineate the relations between goods and plants, and between goods and warehouses, respectively. For any two goods $v_i, v_j \in V_{\mathrm{G}}$, $A_{\mathrm{P},ij}^{(\mathrm{G})} = 1$ if there exists at least one plant v_j such that $(v_{i_1}, v_j) \in E$ and $(v_{i_2}, v_j) \in E$; otherwise,$A_{\mathrm{P},ij}^{(\mathrm{G})} = 0$. Similarly, $A_{\mathrm{W}}^{(\mathrm{G})}$, $A_{\mathrm{W},ij}^{(\mathrm{G})} = 1$ if there exists at least one warehouse v_k such that $(v_{i_1}, v_k) \in E$ and $(v_{i_2}, v_k) \in E$; otherwise, $A_{\mathrm{W},ij}^{(\mathrm{G})} = 0$. In a similar manner, we can establish multi-layer networks for plant nodes and warehouse nodes, represented by sets of adjacency matrices $A^{(\mathrm{P})}$ and $A^{(\mathrm{W})}$, respectively. Then, for each type of nodes, the objective is to perform community detection on the projected multi-layer network.

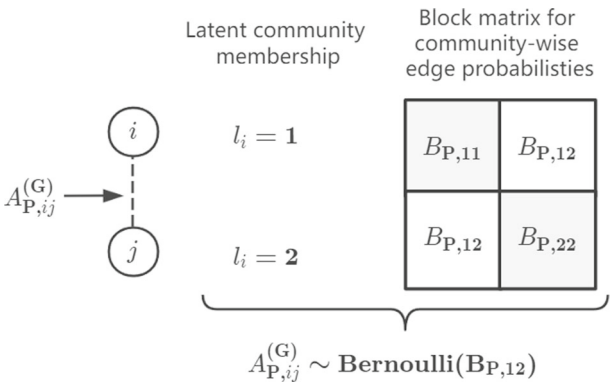

Fig. 2 A toy example of SBM: The assumption related to the element $A^{(G)}_{P,ij}$

2.3 Community detection of projected multi-layer network

Assume that for each type of nodes, there are K underlying communities. In this section, we take the projected network of goods as an example to illustrate the community detection approach for multi-layer networks. Suppose all N_G goods can be categorized into K non-overlapping communities, represented by K index sets $\Psi^{(G)}_1, \ldots, \Psi^{(G)}_K$. For $1 \le k \le K$, the set $\Psi^{(G)}_k$ contains indices of goods belonging to the k-th community. Let $\psi^{(G)} = (\psi^{(G)}_1, \ldots, \psi^{(G)}_{N_G}) \in \{1, \ldots, K\}^{N_G}$ denote the membership vector. For each good $i \in V_G$, $\psi^{(G)}_i = k$ if $i \in \Psi^{(G)}_k$. The objective is to estimate $\psi^{(G)}$ based on $\mathcal{A}^{(G)}$. Regarding community detection in multi-layer networks, it is argued in (Lei et al., 2019) that the least-squares estimator effectively identifies cohesive community structures across layers with robust performance. We adopt the assumptions of the multi-layer stochastic block model (SBM) from Lei et al. (2019) to explore solutions for community detection in the supply chain context. According to SBM, for each element of $A^{(G)}_P$ and $A^{(G)}_W$, which is a binary variable, we assume that it follows a Bernoulli distribution with a corresponding probability parameter. This approach enables us to construct a parametric framework to model $A^{(G)}_P$ and $A^{(G)}_W$, thereby facilitating community detection based on the estimation of these probability parameters. Within the SBM, we assume that the edge probability depends on the latent communities. Specifically, for two latent communities k_1 and k_2, the edge probabilities between any two nodes belonging to the k_1-th and k_2-th communities are identical. We introduce two $K \times K$ symmetric block matrices of community-wise edge probabilities, B_P and B_W, to represent the edge probability parameters for $A^{(G)}_P$ and $A^{(G)}_W$, respectively. For $1 \le i \ne j \le N_G$, we assume $A^{(G)}_{P,ij} \sim \text{Bernoulli}(B_{P,l_1l_2})$ and $A^{(G)}_{W,ij} \sim \text{Bernoulli}(B_{W,l_1l_2})$ when $\psi^{(G)}_i = l_1$ and $\psi^{(G)}_j = l_2$. The parameters B_{P,l_1l_2} and B_{W,l_1l_2} represent the edge densities between nodes from communities l_1 and l_2 in $A^{(G)}_P$ and $A^{(G)}_W$, respectively. To better explain the SBM assumptions, we provide a toy example in Fig. 2, using the element $A^{(G)}_{P,ij}$ for illustration.

Based on multi-layer SBM, consistent estimation can be achieved with a least-squares estimator that minimizes the residual sum of squares as follows:

$$\hat{\psi}^{(G)} = \underset{\psi \in \{1,\ldots,K\}^{N_G}}{\arg\min} \sum_{1 \le i < j \le n} \left\{ \left(A^{(G)}_{W,ij} - \hat{B}^{(G)}_{W,\psi_i\psi_j} \right)^2 + \left(A^{(G)}_{P,ij} - \hat{B}^{(G)}_{P,\psi_i\psi_j} \right)^2 \right\}, \quad (1)$$

where

$$\hat{B}^{(\mathrm{G})}_{\mathrm{W},l_1l_2} = \frac{\sum_{i,j\in\mathcal{S}_l(\psi)} A^{(\mathrm{G})}_{\mathrm{W},ij}}{|\mathcal{S}_l(\psi)|\,(|\mathcal{S}_l(\psi)|-1)}, \hat{B}^{(\mathrm{G})}_{\mathrm{P},l_1l_2} = \frac{\sum_{i,j\in\mathcal{S}_l(\psi)} A^{(\mathrm{G})}_{\mathrm{P},ij}}{|\mathcal{S}_l(\psi)|\,(|\mathcal{S}_l(\psi)|-1)} \text{ when } l_1 = l_2 = l,$$

$$\hat{B}^{(\mathrm{G})}_{\mathrm{W},l_1l_2} = \frac{\sum_{i\in\mathcal{S}_{l_1}(\psi),j\in\mathcal{S}_{l_2}(\psi)} A^{(\mathrm{G})}_{\mathrm{W},ij}}{\left|\mathcal{S}_{l_1}(\psi)\right|\left|\mathcal{S}_{l_2}(\psi)\right|}, \hat{B}^{(\mathrm{G})}_{\mathrm{P},l_1l_2} = \frac{\sum_{i\in\mathcal{S}_{l_1}(\psi),j\in\mathcal{S}_{l_2}(\psi)} A^{(\mathrm{G})}_{\mathrm{P},ij}}{\left|\mathcal{S}_{l_1}(\psi)\right|\left|\mathcal{S}_{l_2}(\psi)\right|} \text{ when } l_1 \neq l_2,$$

with $\mathcal{S}_l(\psi) = \{i : \psi_i = l\}$ and $|\cdot|$ denoting the number of elements within a set. Given a temporal membership vector ϕ and $1 \le l_1 \neq l_2 \le K$, $\hat{B}^{(\mathrm{G})}_{\mathrm{W},l_1l_2}$ is the sample mean of the edge density between communities $\mathcal{S}_{l_1}$ and $\mathcal{S}_{l_2}$. For $1 \le l \le K$, $\hat{B}^{(\mathrm{G})}_{\mathrm{W},ll}$ is the sample mean of the edge density within the community l. With respect to the underlying block matrices B_{P} and B_{W}, for any $1 \le l \le K$, $\hat{B}^{(\mathrm{G})}_{\mathrm{P},l_1l_2}$ and $\hat{B}^{(\mathrm{G})}_{\mathrm{W},l_1l_2}$ serve as consistent estimators of B_{P,l_1l_2} and B_{W,l_1l_2}, respectively. According to the multi-layer SBM, the estimator in (1) is consistent for the membership vector $\phi^{(\mathrm{G})}$. By minimizing the least-squares loss function, the sample means of edge densities tend to approximate the true parameters in B_{P} and B_{W}. Consequently, nodes corresponding to the same underlying community are expected to be assigned to the same communities.

To solve the minimization problem in (1), we consider an approximately equivalent problem, which is illustrated in Lemma 1.

Lemma 1 *For $1 \le l \le K$, suppose that $|\mathcal{S}_l(\psi)|(|\mathcal{S}_l(\psi)|-1) \approx |\mathcal{S}_l(\psi)|^2$ for $1 \le l \le K$. Then, the minimization problem in (1) is equivalent to an maximization problem as follows:*

$$\hat{\psi}^{(\mathrm{G})} = \underset{\psi\in\{1,\ldots,K\}^{N_{\mathrm{G}}}}{\arg\max} \sum_{1\le l_1,l_2\le K} |\mathcal{S}_{l_1}(\psi)||\mathcal{S}_{l_2}(\psi)| \left[\left\{\hat{B}^{(\mathrm{G})}_{\mathrm{W},l_1l_2}\right\}^2 + \left\{\hat{B}^{(\mathrm{G})}_{\mathrm{P},l_1l_2}\right\}^2\right]. \tag{2}$$

Proof To proof this lemma, we decompose the objective function in (1) into two components: $\sum_{1\le i<j\le n}(A^{(\mathrm{G})}_{\mathrm{W},ij} - \hat{B}^{(\mathrm{G})}_{\mathrm{W},\psi_i\psi_j})^2$ and $\sum_{1\le i<j\le n}(A^{(\mathrm{G})}_{\mathrm{P},ij} - \hat{B}^{(\mathrm{G})}_{\mathrm{P},\psi_i\psi_j})^2$. For the first component, we have

$$\begin{aligned}
&2\sum_{1\le i<j\le n}\left(A^{(\mathrm{G})}_{\mathrm{W},ij} - \hat{B}^{(\mathrm{G})}_{\mathrm{W},\psi_i\psi_j}\right)^2 = \sum_{1\le i\neq j\le n}\left(A^{(\mathrm{G})}_{\mathrm{W},ij} - \hat{B}^{(\mathrm{G})}_{\mathrm{W},\psi_i\psi_j}\right)^2 \\
&= \sum_{1\le i\neq j\le n}\left[\left\{A^{(\mathrm{G})}_{\mathrm{W},ij}\right\}^2 - 2A^{(\mathrm{G})}_{\mathrm{W},ij}\hat{B}^{(\mathrm{G})}_{\mathrm{W},\psi_i\psi_j} + \left\{\hat{B}^{(\mathrm{G})}_{\mathrm{W},\psi_i\psi_j}\right\}^2\right] \\
&= \sum_{1\le i\neq j\le n}\left\{A^{(\mathrm{G})}_{\mathrm{W},ij}\right\}^2 + \sum_{1\le l_1,l_2\le K}\sum_{\substack{i\in\mathcal{S}_{l_1}(\psi)\\ j\in\mathcal{S}_{l_2}(\psi)}}\left[-2A^{(\mathrm{G})}_{\mathrm{W},ij}\hat{B}^{(\mathrm{G})}_{\mathrm{W},l_1l_2} + \left\{\hat{B}^{(\mathrm{G})}_{\mathrm{W},l_1l_2}\right\}^2\right] \\
&= \sum_{1\le i\neq j\le n}\left\{A^{(\mathrm{G})}_{\mathrm{W},ij}\right\}^2 + \sum_{1\le l_1,l_2\le K}\sum_{\substack{i\in\mathcal{S}_{l_1}(\psi)\\ j\in\mathcal{S}_{l_2}(\psi)}}\left\{\hat{B}^{(\mathrm{G})}_{\mathrm{W},l_1l_2}\right\}^2 - 2\sum_{1\le l_1,l_2\le K}\hat{B}^{(\mathrm{G})}_{\mathrm{W},l_1l_2}\sum_{\substack{i\in\mathcal{S}_{l_1}(\psi)\\ j\in\mathcal{S}_{l_2}(\psi)}}A^{(\mathrm{G})}_{\mathrm{W},ij} \\
&= \sum_{1\le i\neq j\le n}\left\{A^{(\mathrm{G})}_{\mathrm{W},ij}\right\}^2 - \sum_{1\le l_1\neq l_2\le K}|\mathcal{S}_{l_1}(\psi)||\mathcal{S}_{l_2}(\psi)|\left\{\hat{B}^{(\mathrm{G})}_{\mathrm{W},l_1l_2}\right\}^2 \\
&\quad - \sum_{1\le l\le K}|\mathcal{S}_l(\psi)|(|\mathcal{S}_l(\psi)|-1)\left\{\hat{B}^{(\mathrm{G})}_{\mathrm{W},ll}\right\}^2.
\end{aligned} \tag{3}$$

To simplify the analysis, we adopt the approximation that $|\mathcal{S}_l(\psi)|(|\mathcal{S}_l(\psi)|-1) \approx |\mathcal{S}_l(\psi)|^2$ for $1 \le l \le K$. Then, (3) is approximated as

$$2\sum_{1\le i<j\le n}\left(A^{(\mathrm{G})}_{\mathrm{W},ij}-\hat{B}^{(\mathrm{G})}_{\mathrm{W},\psi_i\psi_j}\right)^2 \approx \sum_{1\le i\ne j\le n}\left\{A^{(\mathrm{G})}_{\mathrm{W},ij}\right\}^2 - \sum_{1\le l_1,l_2\le K}|\mathcal{S}_{l_1}(\psi)||\mathcal{S}_{l_2}(\psi)|\left\{\hat{B}^{(\mathrm{G})}_{\mathrm{W},l_1l_2}\right\}^2.$$

As a result, the maximization of $\sum_{1\le i<j\le n}(A^{(\mathrm{G})}_{\mathrm{W},ij}-\hat{B}^{(\mathrm{G})}_{\mathrm{W},\psi_i\psi_j})^2$ can be approximately implemented by the minimizing $\sum_{1\le l_1,l_2\le K}|\mathcal{S}_{l_1}(\psi)||\mathcal{S}_{l_2}(\psi)|\left\{\hat{B}^{(\mathrm{G})}_{\mathrm{W},l_1l_2}\right\}^2$. For the second component $\sum_{1\le i<j\le n}(A^{(\mathrm{G})}_{\mathrm{P},ij}-\hat{B}^{(\mathrm{G})}_{\mathrm{P},\psi_i\psi_j})^2$, a similar conclusion can be drawn. In summary, we solve (1) through the optimization of an approximately equivalent problem as follows:

$$\hat{\psi}^{(\mathrm{G})} = \underset{\psi\in\{1,\ldots,K\}^{N_\mathrm{G}}}{\arg\max}\sum_{1\le l_1,l_2\le K}|\mathcal{S}_{l_1}(\psi)||\mathcal{S}_{l_2}(\psi)|\left[\left\{\hat{B}^{(\mathrm{G})}_{\mathrm{W},l_1l_2}\right\}^2+\left\{\hat{B}^{(\mathrm{G})}_{\mathrm{P},l_1l_2}\right\}^2\right].$$

□

For Lemma 1, the approximation $|\mathcal{S}_l(\psi)|(|\mathcal{S}_l(\psi)|-1) \approx |\mathcal{S}_l(\psi)|^2$ for $1 \le l \le K$ can be easily achieved in practice, particularly when the number of nodes within each cluster is sufficiently large. Next, we investigate the calculation of the partition based on (2). Given an alternative membership vector $\psi \in \{1,\ldots,K\}^{N_\mathrm{G}}$, we further derive K binary vectors $\Phi^{(\mathrm{G})}_1(\psi),\ldots,\Phi^{(\mathrm{G})}_K(\psi)$, each of which is a $N_\mathrm{G}\times 1$ vector. For $1\le k\le K$ and $1\le i\le N_\mathrm{G}$, $\Phi^{(\mathrm{G})}_{k,i}(\psi)=1$ if $\psi_i=k$, otherwise $\Phi^{(\mathrm{G})}_{k,i}(\psi)=0$. Based on these binary membership vectors, we express $\hat{B}^{(\mathrm{G})}_{\mathrm{W},l_1l_2}$ and $\hat{B}^{(\mathrm{G})}_{\mathrm{P},l_1l_2}$ as $\{|\mathcal{S}_{l_1}(\psi)||\mathcal{S}_{l_2}(\psi)|\}^{-1}\{\Phi^{(\mathrm{G})}_{l_1}(\psi)\}^\top A^{(\mathrm{G})}_\mathrm{W}\Phi^{(\mathrm{G})}_{l_2}(\psi)$ and $\{|\mathcal{S}_{l_1}(\psi)||\mathcal{S}_{l_2}(\psi)|\}^{-1}\{\Phi^{(\mathrm{G})}_{l_1}(\psi)\}^\top A^{(\mathrm{G})}_\mathrm{P}\Phi^{(\mathrm{G})}_{l_2}(\psi)$, respectively. Thus, (2) can be rewritten as

$$\begin{aligned}
\hat{\psi}^{(\mathrm{G})} &= \underset{\psi\in\{1,\ldots,K\}^{N_\mathrm{G}}}{\arg\max}\sum_{1\le l_1,l_2\le K}\frac{1}{|\mathcal{S}_{l_1}(\psi)||\mathcal{S}_{l_2}(\psi)|}\left[\left[\left\{\Phi^{(\mathrm{G})}_{l_1}(\psi)\right\}^\top A^{(\mathrm{G})}_\mathrm{W}\Phi^{(\mathrm{G})}_{l_2}(\psi)\right]^2\right.\\
&\quad\left.+\left[\left\{\Phi^{(\mathrm{G})}_{l_1}(\psi)\right\}^\top A^{(\mathrm{G})}_\mathrm{P}\Phi^{(\mathrm{G})}_{l_2}(\psi)\right]^2\right]\\
&= \underset{\psi\in\{1,\ldots,K\}^{N_\mathrm{G}}}{\arg\max}\sum_{1\le l_1,l_2\le K}\left[\left[\left\{\widetilde{\Phi}^{(\mathrm{G})}_{l_1}(\psi)\right\}^\top A^{(\mathrm{G})}_\mathrm{W}\widetilde{\Phi}^{(\mathrm{G})}_{l_2}(\psi)\right]^2\right.\\
&\quad\left.+\left[\left\{\widetilde{\Phi}^{(\mathrm{G})}_{l_1}(\psi)\right\}^\top A^{(\mathrm{G})}_\mathrm{P}\widetilde{\Phi}^{(\mathrm{G})}_{l_2}(\psi)\right]^2\right]\\
&= \underset{\psi\in\{1,\ldots,K\}^{N_\mathrm{G}}}{\arg\max}\left\|\left\{\widetilde{\Phi}^{(\mathrm{G})}(\psi)\right\}^\top A^{(\mathrm{G})}_\mathrm{W}\widetilde{\Phi}^{(\mathrm{G})}(\psi)\right\|^2_F+\left\|\left\{\widetilde{\Phi}^{(\mathrm{G})}(\psi)\right\}^\top A^{(\mathrm{G})}_\mathrm{P}\widetilde{\Phi}^{(\mathrm{G})}(\psi)\right\|^2_F,
\end{aligned}\tag{4}$$

where $\widetilde{\Phi}^{(\mathrm{G})}(\psi)=[\widetilde{\Phi}^{(\mathrm{G})}_1(\psi),\ldots,\widetilde{\Phi}^{(\mathrm{G})}_K(\psi)]$ is a $N_\mathrm{G}\times K$ matrix with $\widetilde{\Phi}^{(\mathrm{G})}_k(\psi)=\Phi^{(\mathrm{G})}_k(\psi)/\sqrt{|\mathcal{S}_k(\psi)|}$ for $k=1,\ldots,K$. According to (4), we further conclude that the solution of (2) can be obtained by the spectral clustering method. The result is given in the following theorem.

Theorem 1 *The maximization problem in (2) is approximately equivalent to a spectral clustering problem as follows:*

$$\widehat{\Phi}^{(\mathrm{G})} = \underset{\Phi\in\mathbf{R}^{N_\mathrm{G}\times K},\Phi^\top\Phi=I_K}{\arg\max}\ \mathrm{trace}\left(\Phi^\top\left[\left\{A_\mathrm{W}^{(\mathrm{G})}\right\}^2+\left\{A_\mathrm{P}^{(\mathrm{G})}\right\}^2\right]\Phi\right).$$

Proof Note that for $1\le l_1\ne l_2\le K$, we have $\{\widetilde{\Phi}_{l_1}^{(\mathrm{G})}(\psi)\}^\top\widetilde{\Phi}_{l_2}^{(\mathrm{G})}(\psi)=0$. Moreover, for $1\le k\le K$, $\{\widetilde{\Phi}_k^{(\mathrm{G})}(\psi)\}^\top\widetilde{\Phi}_k^{(\mathrm{G})}(\psi)=1$. Therefore, $\{\widetilde{\Phi}_1^{(\mathrm{G})}(\psi),\ldots,\widetilde{\Phi}_K^{(\mathrm{G})}(\psi)\}$ is a group of orthogonal vectors and $\widetilde{\Phi}^{(\mathrm{G})}(\psi)$ is an orthogonal matrix with $\{\widetilde{\Phi}^{(\mathrm{G})}(\psi)\}^\top\widetilde{\Phi}^{(\mathrm{G})}(\psi)=I_K$, where I_K is the K-order identity matrix. For the orthogonal matrix $\widetilde{\Phi}^{(\mathrm{G})}$ and the symmetric matrices $A_\mathrm{W}^{(\mathrm{G})}$ and $A_\mathrm{P}^{(\mathrm{G})}$, we have

$$\begin{aligned}
&\left\|\left\{\widetilde{\Phi}^{(\mathrm{G})}(\psi)\right\}^\top A_\mathrm{W}^{(\mathrm{G})}\widetilde{\Phi}^{(\mathrm{G})}(\psi)\right\|_F^2+\left\|\left\{\widetilde{\Phi}^{(\mathrm{G})}(\psi)\right\}^\top A_\mathrm{P}^{(\mathrm{G})}\widetilde{\Phi}^{(\mathrm{G})}(\psi)\right\|_F^2\\
&\quad=\mathrm{trace}\left(\left\{\widetilde{\Phi}^{(\mathrm{G})}(\psi)\right\}^\top A_\mathrm{W}^{(\mathrm{G})}\widetilde{\Phi}^{(\mathrm{G})}(\psi)\left\{\widetilde{\Phi}^{(\mathrm{G})}(\psi)\right\}^\top A_\mathrm{W}^{(\mathrm{G})}\widetilde{\Phi}^{(\mathrm{G})}(\psi)\right)\\
&\qquad+\mathrm{trace}\left(\left\{\widetilde{\Phi}^{(\mathrm{G})}(\psi)\right\}^\top A_\mathrm{P}^{(\mathrm{G})}\widetilde{\Phi}^{(\mathrm{G})}(\psi)\left\{\widetilde{\Phi}^{(\mathrm{G})}(\psi)\right\}^\top A_\mathrm{P}^{(\mathrm{G})}\widetilde{\Phi}^{(\mathrm{G})}(\psi)\right)\\
&\quad\le\mathrm{trace}\left(\left\{\widetilde{\Phi}^{(\mathrm{G})}(\psi)\right\}^\top\left\{A_\mathrm{W}^{(\mathrm{G})}\right\}^2\widetilde{\Phi}^{(\mathrm{G})}(\psi)\right)+\mathrm{trace}\left(\left\{\widetilde{\Phi}^{(\mathrm{G})}(\psi)\right\}^\top\left\{A_\mathrm{P}^{(\mathrm{G})}\right\}^2\widetilde{\Phi}^{(\mathrm{G})}(\psi)\right)\\
&\quad=\mathrm{trace}\left(\left\{\widetilde{\Phi}^{(\mathrm{G})}(\psi)\right\}^\top\left[\left\{A_\mathrm{W}^{(\mathrm{G})}\right\}^2+\left\{A_\mathrm{P}^{(\mathrm{G})}\right\}^2\right]\widetilde{\Phi}^{(\mathrm{G})}(\psi)\right).
\end{aligned}\tag{5}$$

The inequality in (5) becomes equality when $A_\mathrm{W}^{(\mathrm{G})}$ and $A_\mathrm{P}^{(\mathrm{G})}$ share the same community structure and $\widetilde{\Phi}^{(\mathrm{G})}(\psi)$ comprises eigenvectors corresponding to the leading K eigenvalues of $\{A_\mathrm{W}^{(\mathrm{G})}\}^2+\{A_\mathrm{P}^{(\mathrm{G})}\}^2$. Therefore, to maximize the objective function in (4), it suffices to search for an estimation $\hat{\psi}^{(\mathrm{G})}$ satisfying $\widetilde{\Phi}^{(\mathrm{G})}(\hat{\psi}^{(\mathrm{G})})=\widehat{\Phi}^{(\mathrm{G})}$, where

$$\widehat{\Phi}^{(\mathrm{G})} = \underset{\Phi\in\mathbf{R}^{N_\mathrm{G}\times K},\Phi^\top\Phi=I_K}{\arg\max}\ \mathrm{trace}\left(\Phi^\top\left[\left\{A_\mathrm{W}^{(\mathrm{G})}\right\}^2+\left\{A_\mathrm{P}^{(\mathrm{G})}\right\}^2\right]\Phi\right).\tag{6}$$

However, due to the constraint $\hat{\psi}^{(\mathrm{G})}\in\{1,\ldots,K\}^{N_\mathrm{G}}$, this computation may be costly in practice. To address this issue, community detection is conducted in a two-step manner.

Step 1 To solve the optimization problem in (6) and obtain $\widehat{\Phi}^{(\mathrm{G})}$, we initially ignore the restriction on $\hat{\psi}^{(\mathrm{G})}$. Then, we investigate $[\{A_\mathrm{W}^{(\mathrm{G})}\}^2+\{A_\mathrm{P}^{(\mathrm{G})}\}^2]$ through eigenvalue decomposition.

Step 1.1 Conduct the eigenvalue decomposition of $[\{A_\mathrm{W}^{(\mathrm{G})}\}^2+\{A_\mathrm{P}^{(\mathrm{G})}\}^2]$. The decomposition leads to $[\{A_\mathrm{W}^{(\mathrm{G})}\}^2+\{A_\mathrm{P}^{(\mathrm{G})}\}^2]=U^\top\Sigma U$, where $\Sigma=\mathrm{diag}(\lambda_1,\ldots,\lambda_{N_\mathrm{G}})$ is a diagonal matrix comprising N_G eigenvalues and U is the corresponding $N_\mathrm{G}\times N_\mathrm{G}$ eigenvector matrix.

Step 1.2 Find the K largest eigenvalues. Let $\lambda_{(1)},\ldots,\lambda_{(K)}$ denote the K largest eigenvalues. For $\lambda_{(k)}$, $1\le k\le K$,let $u_k\in\mathbf{R}^{N_\mathrm{G}}$ denote the corresponding eigenvector.

Step 1.3 Compile an $N_\mathrm{G}\times K$ eigenvector matrix. Let U_K denote the eigenvector matrix with $U_K=[u_1^\top,\ldots,u_K^\top]$. It follows that the estimation $\widehat{\Phi}^{(\mathrm{G})}$ from (6) equals U_K. Hence, $\widehat{\Phi}^{(\mathrm{G})}$ can be viewed as a spectral embedding of $[\{A_\mathrm{W}^{(\mathrm{G})}\}^2+\{A_\mathrm{P}^{(\mathrm{G})}\}^2]$. Thus, we directly compute $\widehat{\Phi}^{(\mathrm{G})}$ by the spectral decomposition of $[\{A_\mathrm{W}^{(\mathrm{G})}\}^2+\{A_\mathrm{P}^{(\mathrm{G})}\}^2]$.

Step 2 To partition the N_G goods, we adopt classic clustering algorithms, e.g., the K-means algorithm, to the rows of $\widehat{\Phi}^{(\mathrm{G})}$. The resulting partition is the final estimation for the membership vector. □

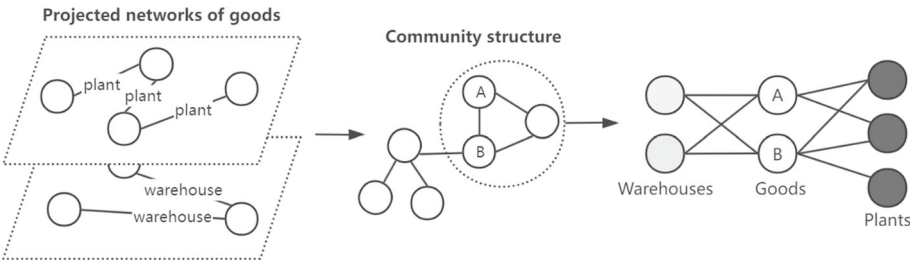

Fig. 3 Relationships in production capacity among objects within the same community

Theorem 1 paves the way for a cost-efficient solution to address equation (2). Leveraging this theorem, we are enabled to implement community detection within multi-layer networks by employing the classic spectral clustering algorithm, as shown in the aforementioned steps 1 and 2. This multi-layer community detection approach is referred to as MLCD for short. To illustrate the process of MLCD in detail, we take the community detection for goods as an example and summarize all steps, including the detailed steps of computing spectral embeddings, in Algorithm 1.

Algorithm 1 MLCD algorithm

Input: K: number of communities; $\mathcal{A}^{(\mathrm{G})} = \{A_{\mathrm{P}}^{(\mathrm{G})}, A_{\mathrm{W}}^{(\mathrm{G})}\}$: projected multi-layer network of goods;
Compute an aggregated matrix $\widetilde{A} = \{A_{\mathrm{W}}^{(\mathrm{G})}\}^2 + \{A_{\mathrm{P}}^{(\mathrm{G})}\}^2$;
for $i \in \{1, \ldots, N_{\mathrm{G}}\}$ **do**
  Set the diagonal element $\widetilde{A}_{ii}$ to be 0;
end for
Initialize an $N_{\mathrm{G}} \times N_{\mathrm{G}}$ zero matrix $\widetilde{D}$;
for $i \in \{1, \ldots, N_{\mathrm{G}}\}$ **do**
  $\widetilde{D}_{ii} = \sum_{j=1}^{N_{\mathrm{G}}} \widetilde{A}_{ij}$;
end for
Compute a Laplacian matrix $L = \widetilde{D}^{-\frac{1}{2}} \widetilde{A} \widetilde{D}^{-\frac{1}{2}}$;
Find the K largest eigenvalues of L and the corresponding eigenvectors. Stack the eigenvectors to form an $N_{\mathrm{G}} \times K$ matrix $\widehat{V}$;
Apply K-means method to cluster the N_{G} rows of $\widehat{V}$ into K clusters. Because each row of $\widehat{V}_n$ refers to an individual good node, the result of K-means clustering leads to an estimation of the membership vector of goods $\hat{\psi}^{(\mathrm{G})}$.
Output: An estimation of the membership vector of goods $\hat{\psi}^{(\mathrm{G})}$.

For plants and warehouses, we perform community detection similarly. We generate projected multi-layer networks based on plants and warehouses, respectively. Then, we estimate the membership vectors using the aforementioned two steps.

Remark 1. From the perspective of community detection, the networks need to be acyclic. Specifically, for any $N \times N$ adjacency matrix A, it is required $A_{ii} = 0$ for any $1 \leq i \leq N$. For the aggregated network $[\{A_{\mathrm{W}}^{(\mathrm{G})}\}^2 + \{A_{\mathrm{P}}^{(\mathrm{G})}\}^2]$, we conduct a sweeping operation to set the diagonal elements to be 0. In this way, we ensure the networks in our analysis framework are acyclic.

Based on the results of community detection, we identify distinct clusters for plants, plants, and warehouses. Each cluster comprises entities with strong implicit relationships. From the perspective of supply chain management, entities within the same cluster exhibit overlapping

production capacities. Production capacity can be readily shifted between objects in the same cluster. For example, consider the case illustrated in Fig. 3. The clustering result indicates that goods A and B belong to the same local community. They are assigned to the same cluster because multiple plants can produce both of them, and many warehouses can store them simultaneously. Consequently, if the supply of good A is disrupted by external factors, the supply chain manager can quickly restore its production capacity by utilizing the plants and warehouses associated with good B. In this way, the identified community structure can be leveraged to explore the flexibility and redundancy among goods, plants, and warehouses.

3 Simulation study

To test the performance of the multi-layer community detection method for supply chains, we conduct a simulation study based on simulated networks of supply chains. Specifically, we generate simulated datasets based on SBM with multi-mode nodes. The number of communities is set to be $K = 3$. For $1 \le i \le N$, the community label of node i, which is denoted a l_i, is randomly picked from $\{1, 2, 3\}$. Each community consists of nodes of three types: good, plant, and warehouse. Let $\mathrm{G}_1, \mathrm{G}_2, \mathrm{G}_3$ represent the nodes corresponding to goods in the 1st, 2nd, and 3rd communities, respectively. Then, let $P_{\mathrm{G}_{k_1},\mathrm{G}_{k_2}}$ denote the edge density between any two nodes belonging to the sets G_{k_1} and G_{k_2}, respectively. In a similar manner, we use $\mathrm{P}_1, \mathrm{P}_2, \mathrm{P}_3$ and $\mathrm{W}_1, \mathrm{W}_2, \mathrm{W}_3$ to represent the nodes corresponding to plants and warehouses, respectively. The block matrix of our multi-mode network is defined as

$$B = \begin{bmatrix} B_{11} & B_{12} & B_{13} \\ B_{12} & B_{22} & B_{23} \\ B_{13} & B_{23} & B_{33} \end{bmatrix} \in \mathbf{R}^{9\times 9},$$

where for $k_1, k_2 \in \{1, 2, 3\}$,

$$B_{k_1k_2} = \begin{bmatrix} P_{\mathrm{G}_{k_1},\mathrm{G}_{k_2}} & P_{\mathrm{G}_{k_1},\mathrm{P}_{k_2}} & P_{\mathrm{G}_{k_1},\mathrm{W}_{k_2}} \\ P_{\mathrm{P}_{k_1},\mathrm{G}_{k_2}} & P_{\mathrm{P}_{k_1},\mathrm{P}_{k_2}} & P_{\mathrm{P}_{k_1},\mathrm{W}_{k_2}} \\ P_{\mathrm{W}_{k_1},\mathrm{G}_{k_2}} & P_{\mathrm{W}_{k_1},\mathrm{P}_{k_2}} & P_{\mathrm{W}_{k_1},\mathrm{W}_{k_2}} \end{bmatrix} \in \mathbf{R}^{3\times 3}.$$

The edge probabilities for nodes with the same mode are supposed to be 0. Thus, for any $k_1, k_2 \in \{1, 2, 3\}$, $P_{\mathrm{G}_{k_1},\mathrm{G}_{k_2}}$, $P_{\mathrm{P}_{k_1},\mathrm{P}_{k_2}}$ and $P_{\mathrm{W}_{k_1},\mathrm{W}_{k_2}}$ are all set to be 0. To simplify the setting, we use P_{innner} and P_{outer} to denote the probability of an edge between two nodes within the same community and that between nodes from different communities. For $k \in \{1, 2, 3\}$, we set $P_{\mathrm{G}_k,\mathrm{P}_k} = P_{\mathrm{G}_k,\mathrm{W}_k} = P_{\mathrm{P}_k,\mathrm{W}_k} = P_{\text{inner}}$. For any $k_1 \ne k_2$, we set $P_{\mathrm{G}_{k_1},\mathrm{P}_{k_2}} = P_{\mathrm{G}_{k_1},\mathrm{W}_{k_2}} = P_{\mathrm{P}_{k_1},\mathrm{W}_{k_2}} = P_{\text{outer}}$. To model the community structure, P_{innner} is set to 10 times of P_{outer}. Based on B and the randomly generated community labels, we can generate an $N \times N$ binary adjacency matrix A to simulate a comprehensive multi-mode network of a supply chain. For any two nodes, whether there will be an edge between them is a Bernoulli event. The matrix A is initialized with all elements being 0. Then, for $1 \le i \ne j \le N$ with $l_i = l_j$, A_{ij} will be updated to 1 with the probability P_{inner}. For $1 \le i \ne j \le N$ with $l_i \ne l_j$, $A_{ij} = 1$ with the probability P_{outer}. Given A, we can project it into single-mode multi-layer networks (e.g., $\mathcal{A}^{(\mathrm{G})} = \{A_{\mathrm{P}}^{(\mathrm{G})}, A_{\mathrm{W}}^{(\mathrm{G})}\}$) and then apply the above-mentioned MLCD approach. To evaluate the performance of MLCD, we consider the following baseline methods.

- Single-layer community detection (SLCD): Conduct community detection with the standard spectral clustering algorithm using only one layer selected from the project networks.

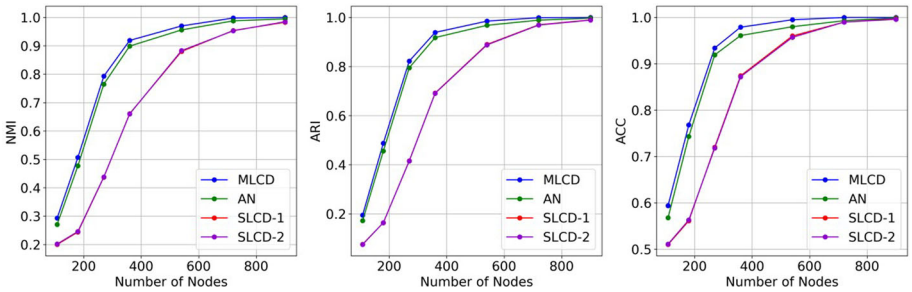

Fig. 4 Performances of different community detection methods for $P_{\text{inner}} = 0.1$

- Community detection on aggregated network (AN): Aggregate multiple layers by directly summing the corresponding adjacency matrices. Then, conduct community detection with the standard spectral clustering algorithm using the aggregated matrix.

With respect to the evaluation criterion, we employ the commonly used criterion for clustering, including Normalized Mutual Information (NMI), Adjusted Rand Index (ARI) and Accuracy based on Hungary algorithm (ACC), to measure the community detection performance. To robustly measure the clustering performances, we report the averaged results over 300 random replications.

3.1 Numerical results

To emulate real supply chains, we established two distinct scenarios based on the edge probability P_{inner}. Specifically, we set P_{inner} to 0.1 and 0.03. These configurations are designed to emulate supply chain networks with varying degrees of sparsity. A lower value of P_{inner} indicates a sparser network, implying fewer connections between the nodes within a supply chain.

The simulation results for $P_{\text{inner}} = 0.1$ are presented in Fig. 4, using the results from a multi-layer network of goods for visualization. For SLCD, community detection based on the projected single-layer network of plants is denoted as SLCD-1, while that based on the projected single-layer network of warehouses is denoted as SLCD-2. In our simulation, since the edge probabilities between nodes with different modes are uniformly configured, the performances of SLCD-1 and SLCD-2 are highly similar. We report community detection results for networks of goods with varying numbers of nodes N. Similar results have been obtained for the multi-layer networks of plants and warehouses. From Fig. 4, we derive several key conclusions. First, MLCD consistently demonstrates superior performance across different network sizes, particularly excelling at larger scales. Second, the results show that for MLCD, community detection performance improves with increasing network size, as measured by NMI, ARI, and ACC. This underscores the effectiveness of MLCD in capturing complex relationships within large-scale networks. Third, SLCD performs less effectively compared to MLCD and AN, suggesting that relying solely on a single network layer for community detection significantly limits performance. The results demonstrate that the integration of multiple layers enhances the detection of densely connected regions in supply chains.

To further assess the performance of MLCD in sparse network structures, we present simulation results with $P_{\text{inner}} = 0.03$ in Fig. 5. Similar to the results for $P_{\text{inner}} = 0.1$, MLCD demonstrates advantages over other methods across various network sizes. It is noteworthy

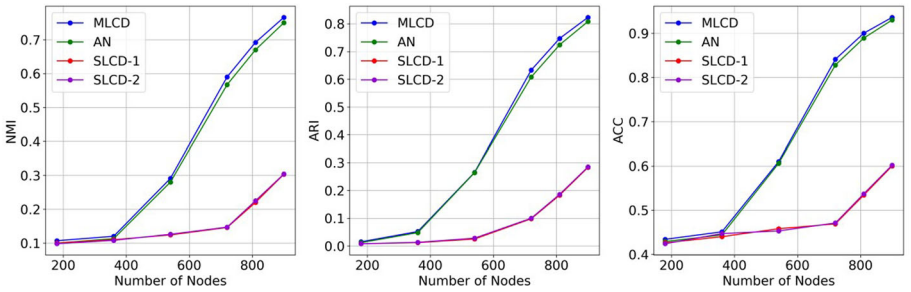

Fig. 5 Performances of different community detection methods for $P_{\text{inner}} = 0.03$

that, for a given number of nodes N, MLCD performs better when the network structure is relatively dense. In the case of sparse networks, MLCD requires more network information, which often correspond to larger network sizes, to achieve robust detection performance.

4 Empirical study

In this section, we demonstrate the effectiveness of the proposed method through an empirical study using a real dataset from a supply chain. The dataset is sourced from the central database system of one of the largest Fast Moving Consumer Goods (FMCG) companies in Bangladesh (Wasi et al., 2023). Due to commercial sensitivity, the dataset does not include actual good names, good codes, or company names. It spans the period from January 1, 2023, to August 9, 2023, and includes three types of nodes: goods, plants, and warehouses. The company's operations extend across the entirety of Bangladesh. Figure 6 presents a visualization of the multi-mode network, illustrating the resilience of the supply chain through its network density. Nodes represent different goods, plants, and warehouses, and are color-coded to distinguish node types. Edges depict various relationships connecting these nodes, such as goods being produced in plants or stored in warehouses. The multi-mode network density of 0.363 indicates a medium level of connectivity, suggesting that the network is neither sparse nor overly dense. For a more comprehensive understanding, further analysis should consider factors such as the arrangement and structure of nodes.

By analyzing this dataset, we can gain a profound understanding of the company's production and storage network, providing a solid foundation for supply chain resilience analysis. In the following part, we investigate the projected single-model network of goods and plants, respectively, to explore the redundancy and flexibility within the supply chain.

4.1 Projected network of goods

To begin with, we will conduct a resilience analysis on the projected network of goods. By assessing the network's resilience to risks and its recovery capabilities, we can identify potential vulnerabilities and recommend targeted improvement strategies. Goods are the core of the supply chain, serving as the primary objects of consumer demand. They play a crucial role in meeting market needs and bridging the gap between production and consumption. Managing goods involves maintaining optimal inventory levels, accurately forecasting sales, and effectively responding to demand fluctuations. Precise management of goods can reduce inventory costs, prevent shortages or overstocking, and enhance the supply chain's respon-

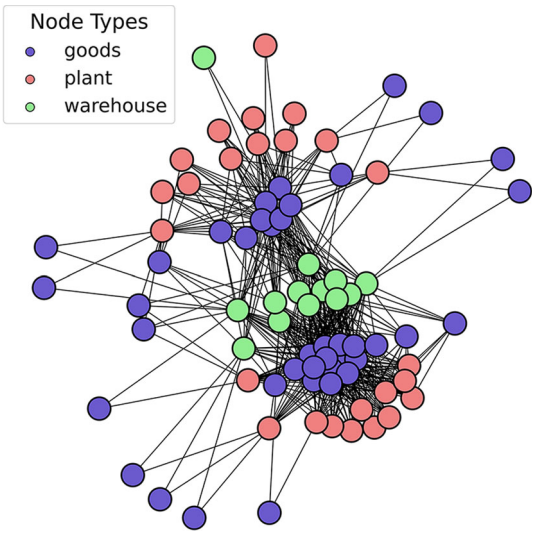

Fig. 6 multi-mode supply chain network

Table 2 Descriptive information of the projected network of goods

	Edge count	Network density	Clustering coefficient
Plant layer	360	0.462	0.436
Warehouse layer	665	0.853	0.708

siveness and flexibility. As described in Sect. 2, the indirect relations form a single-mode network of goods with both plant and warehouse layers. Inspired by Inverse Document Frequency (IDF), we calculate the inverse of the number of goods corresponding to each plant and warehouse. For each pair of goods nodes, the minimum value of these inverses is taken as the edge weight. Table 2 provides detailed information about the projected network of goods. A network density of 0.462 indicates a moderate level of connectivity within the plant layer network, suggesting numerous connections between nodes. This implies that many goods may share resources, processes, or production lines during manufacturing. A weighted clustering coefficient of 0.436 indicates the presence of relatively tight-knit small groups or clusters within the plant layer, showing strong production-related associations among the goods within these clusters. The network density and weighted clustering coefficient for the warehouse layer are both relatively high, indicating a high number of connections among the goods nodes within the network. This suggests that many goods likely have similar storage or processing needs in the warehouse, leading to a robust local clustering structure. These goods are not only interconnected but also exhibit a notably high intensity of interrelations, especially within the Warehouse layer.

Community detection on the projected multi-layer network of goods produces the results depicted in Fig. 7. The image visually represents the structure of the multi-layer network by rearranging the order of goods in the adjacency matrix. It is evident that two distinct goods communities were detected, indicating the presence of two separate groups within the network.

The clustering results offer valuable insights, revealing the hidden relationships among goods within the supply chain network. Goods clustered into the same community often share

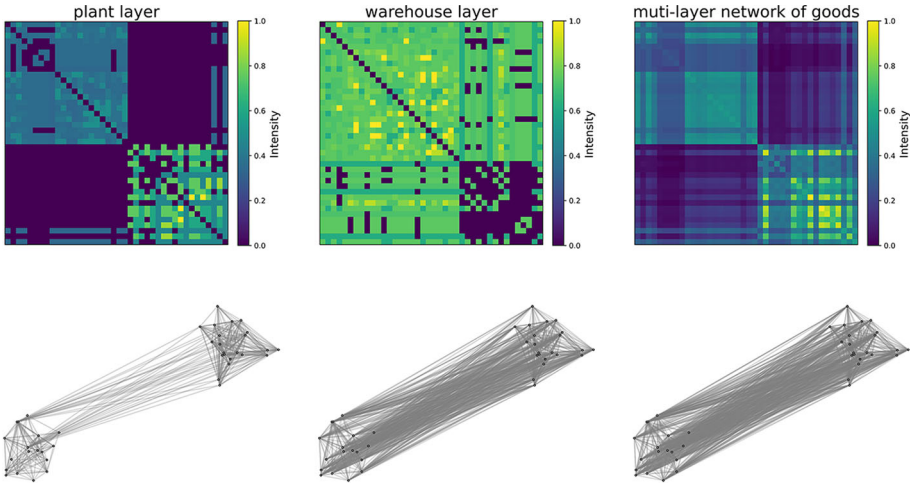

Fig. 7 The adjacency matrices of goods in the plant layer and warehouse layer (top row) and their corresponding networks (bottom row)

significant overlaps in the plants and warehouses they utilize. This finding has substantial implications for supply chain management, as identifying goods communities can enhance risk management and improve supply chain flexibility. By recognizing these communities, companies can develop contingency plans for critical goods to ensure that disruptions at individual nodes (plants or warehouses) do not cripple the entire supply chain. For instance, if goods A and B are within the same community and the plant or warehouse for good A becomes unavailable, a replacement can be sourced from the plant or warehouse for good B. This coordination enhances capacity management and bolsters the supply chain's flexibility and responsiveness.

Beyond enhancing supply chain resilience, community detection of goods can significantly optimize inventory management by minimizing redundant stock and reducing holding costs. Additionally, it can lead to cost efficiencies through streamlined transportation and distribution processes. By consolidating shipments of commonly grouped goods, transportation costs are lowered, and delivery times are improved. This synchronization of plant and warehouse operations leads to overall efficiency improvements.

During the COVID-19 pandemic, many companies faced supply chain disruptions. Companies with a clear understanding of the overlapping goods between plants and warehouses were better positioned to adapt swiftly by reallocating inventory and resources to meet changing demands. For example, a company aware of the availability of critical medical supplies at both manufacturing plants and distribution centers could ensure a continuous supply to hospitals and clinics, even when some nodes were affected by lockdowns or supply delays.

Figure 8 illustrates the network structures of the two communities derived from the clustering results. The edges signify relationships among the plants, such as shared plant or storage locations, shared raw material requirements, product interdependencies, and other influencing factors. Cluster 1 demonstrates a denser and more interconnected structure compared to Cluster 2. Table 3 provides the network density and clustering coefficients for both communities across the plant and warehouse layers after post-clustering.

After clustering, the first cluster shows an increase in both the weighted clustering coefficient and network density, indicating a tighter internal structure. This improved structure

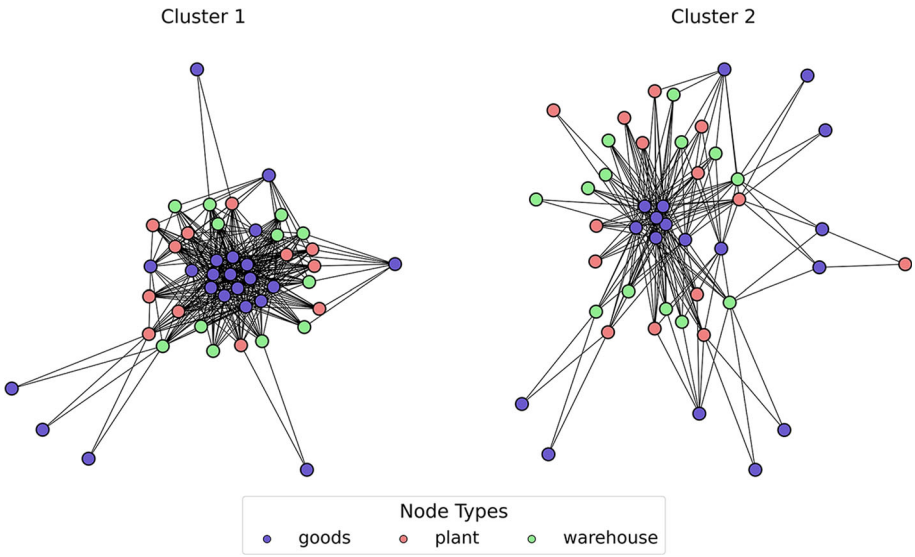

Fig. 8 2 clusters within the projected network of goods

Table 3 Descriptive information of 2 clusters of goods

Network density			
Plant layer	0.462	Warehouse layer	0.853
Cluster 1 (Plant layer)	0.918	Cluster 1 (Warehouse layer)	0.918
Cluster 2 (Plant layer)	0.758	Cluster 2 (Warehouse layer)	0.797
Clustering coefficient			
Plant layer	0.436	Warehouse layer	0.708
Cluster 1 (Plant layer)	0.756	Cluster 1 (Warehouse layer)	0.775
Cluster 2 (Plant layer)	0.556	Cluster 2 (Warehouse layer)	0.648

fosters more efficient internal communication and resource allocation. In contrast, the second cluster experiences a slight decrease in its clustering coefficient and network density, suggesting looser connections and collaborations among its nodes. This may indicate greater independence among the nodes.

(1) Flexibility Analysis of goods

Flexibility in the supply chain refers to the ability to swiftly adapt to market demand fluctuations or other uncertainties, highlighting the system's responsiveness and adaptability in a dynamic environment.

Manufacturing a good across multiple plants allows production tasks to be quickly transferred to alternative facilities if issues arise at one plant, such as equipment failure or raw material shortages. This ensures production continuity and stability. Therefore, the more plants and warehouses associated with a good, the more quickly production plans, supply chain strategies, and logistics arrangements can be adjusted to meet market demand changes. For example, in the event of a sudden surge in order volume, plants can flexibly allocate

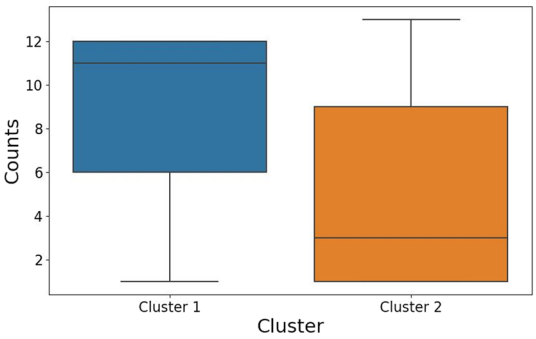

Fig. 9 The number of plants associated with goods for different clusters

resources, reduce production switching time and costs, and enhance production response speed.

In the schematic diagram, goods nodes positioned farther from the network center are associated with fewer plants or warehouses, indicating reduced flexibility. Cluster 1 has 5 goods nodes located relatively outward, while Cluster 2 has 8. This observation suggests that the supply chain flexibility of goods in Cluster 1 is greater. This hypothesis of stronger supply chain flexibility in Cluster 1 is supported by descriptive statistics and box plots comparing the number of plants associated with different categories of goods, as depicted in Fig. 9, which visually illustrates the variations in flexibility among different categories of goods. This is achieved through box plots that depict the number of plants associated with each category. Since the number of warehouses corresponds to the number of plants for each good, separate displays for warehouses are omitted.

Cluster 1 demonstrates an average association of approximately 8 plants and warehouses per good, with the median exceeding 10, indicating robust production and storage flexibility. This abundance of production facilities and storage sites allows for wider dispersion, facilitating swift adjustments in production and distribution plans during emergencies such as natural disasters, equipment failures, or logistics disruptions, thereby ensuring supply chain continuity. Moreover, the diverse array of plants and warehouses enables goods in this category to adeptly navigate fluctuations and shifts in market demand. Conversely, goods in Cluster 2, with relatively fewer plants and warehouses, demonstrate weaker supply chain resilience. The concentration of production facilities and storage locations makes the supply chain more vulnerable to shocks during emergencies, resulting in longer recovery times.

The standard deviation of the number of plants and warehouses for goods in both clusters exceeds 4.5, with minimal variation in minimum values and only a marginal difference of 1 in maximum values. This suggests that while the redundancy in Cluster 1 outperforms that in Cluster 2, managers must remain attentive to supply chain dynamics for certain goods and implement targeted measures such as strategic holiday planning and dynamic adjustments to product rates. Specific recommendations will be detailed in subsequent sections.

To illustrate the differences in flexibility more intuitively, we use the local network of a node as an example, as depicted in Fig. 10. The flexibility of the goods node SOS005L04P in Cluster 1 surpasses that of MAR02K12P in Cluster 2 by a factor of 4.

(2) Redundancy Analysis of goods

Redundancy in a supply chain involves integrating additional resources, inventory, equipment, or capabilities to mitigate potential disruptions or risks. These redundant resources are typically not used in regular operations but can be quickly activated during emergencies.

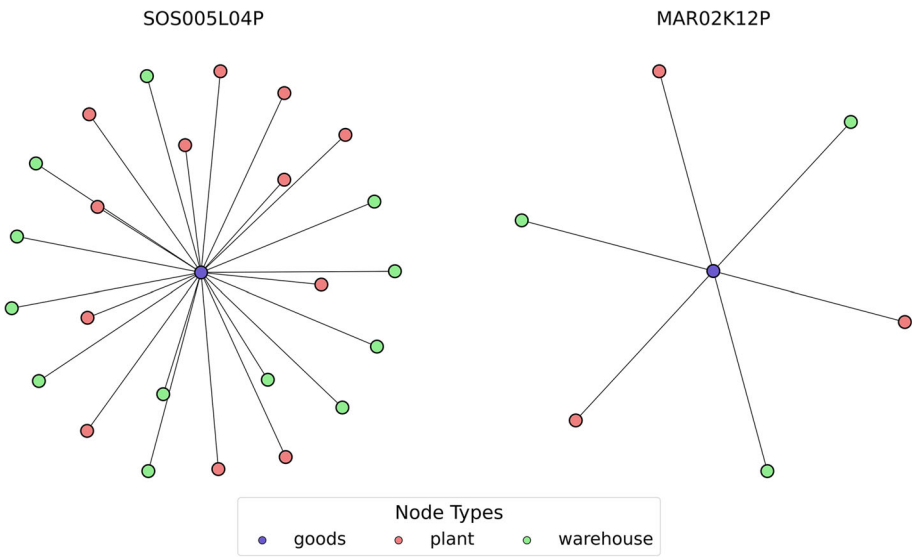

Fig. 10 Local networks of Node SOS005L04P and Node MAR02K12P

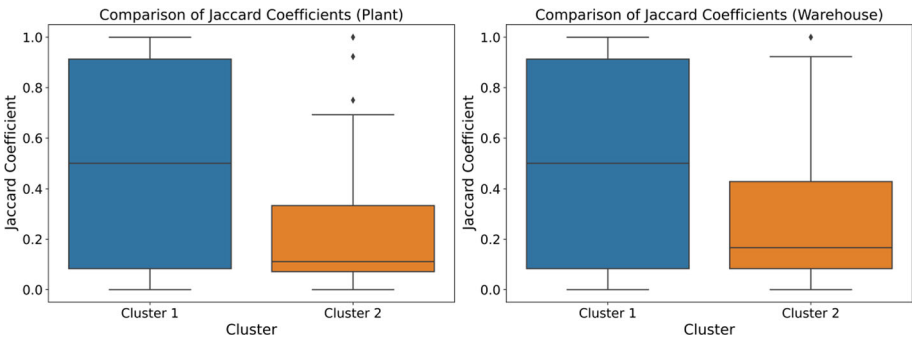

Fig. 11 Jaccard coefficients for good combinations in plants and warehouses

Goods within the same community that share similar production and storage characteristics indicate higher interchangeability and substitutability of supply chain links. This mutual support and supplementation among goods enhance the supply chain's resilience and ability to withstand risks. Identifying highly correlated goods supply chains within a community allows businesses to use them as backup resources. In the event of disruptions, these backup resources can be quickly mobilized to restore production and supply. Therefore, evaluating the degree of shared plants and warehouses among goods within a community helps assess the supply chain's redundancy. This analysis provides insights into the community's capacity to quickly resume normal operations during emergencies and effectively manage supply chain resilience.

The Jaccard coefficient is used to measure the correlation between goods, indirectly indicating the uniqueness of each good and the redundancy within two communities. The comparative results are illustrated in Fig. 11.

Supply chain redundancy involves integrating additional resources, inventory, equipment, or capabilities to address potential disruptions or risks. These redundant resources are generally not utilized in regular operations but can be quickly activated during emergencies. In Cluster 1, the Jaccard coefficients for combinations of goods nodes are evenly distributed between 0 and 1. Conversely, in Cluster 2, the majority of goods nodes combinations exhibit Jaccard coefficients concentrated below 0.5. This lower product correlation within the community indicates more challenging production coordination and reduced supply chain redundancy. To address this issue, implementing regular emergency drills and establishing rapid response teams are essential steps to enhance supply chain resilience management. Through comprehensive analysis, we gain deeper insights into the performance of the goods network in supply chain operations. These insights allow us to propose targeted improvements aimed at boosting resilience and ensuring more robust supply chain management. For the projected network of plants, we conduct a resilience analysis based on multi-layer community detection in the same way. The results are included in the Appendix.

5 Conclusion

Analysis of supply chain resilience is crucial for enterprise production operations and long-term development. In the current complex and volatile economic environment, it is essential to quantify supply chain resilience in terms of flexibility and redundancy. This approach provides valuable insights for maintaining supply chain operations. This study addresses this issue by conducting community detection within the supply chain network. We project the complex supply chain network into single-mode, multi-layer networks focusing on plants and plants. Through multi-layer community detection methods, we identify local units within the network. These closely connected clusters help analyze capacity linkages between different plants and potential coordination among plants. The results reveal the flexibility and redundancy in product manufacturing. Our empirical study, based on a real dataset, demonstrates that applying multi-layer network clustering effectively uncovers indirect capacity linkages between plants and warehouses. The community detection results are valuable for capacity management, strategic allocation, and providing decision-making support for enterprises to handle supply shortages or sudden spikes in demand.

For future research, we plan to test this method on additional supply chain datasets. We will also integrate multi-layer network clustering with capacity forecasting to provide more comprehensive references for analysis of supply chain resilience.

Appendix A Appendix

Appendix A.1 Projected network of plants

After analyzing the goods network, we focus on examining the resilience of the plant network. The robustness of the plant network is crucial for the overall efficiency of the supply chain.

Plants are critical components of the supply chain, responsible for converting raw materials into finished plants. Their primary functions include production planning, manufacturing execution, quality control, and capacity management. The efficiency and flexibility of plant operations directly impact the overall performance of the supply chain. Effective plant management can shorten production cycles, improve product quality, and enhance the supply

Table 4 Descriptive information of the projected network of plants

	Edge count	Network density	Clustering coefficient
Good layer	145	0.483	0.625
Warehouse layer	300	1.000	0.959

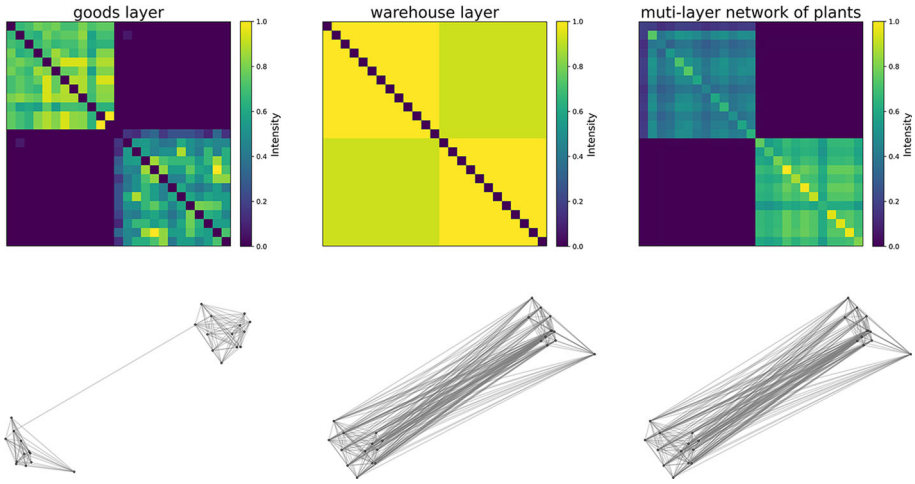

Fig. 12 The adjacency matrices of plants in the good layer and warehouse layer (top row) and their corresponding networks (bottom row)

chain's resilience and responsiveness to market changes. The projected network of plants is a multi-layered structure, constructed based on the production of the same goods and the sharing of the same warehouse as indirect relations. Detailed information on this projected network is provided in Table 4. To analyze the connections within this network, we computed the Jaccard coefficient for each pair of plant nodes, using the intersection over union of goods or warehouses as the basis for the sets, with this value serving as the edge weight. The network density of 0.483 and a weighted clustering coefficient of 0.625 in the goods layer suggest a relatively cohesive structure, although not fully connected. This indicates a strong local clustering tendency, with nodes forming dense subgroups or communities. In contrast, the warehouse layer exhibits both network density and clustering coefficients close to 1.000, reflecting a highly dense and locally clustered network structure.

The community detection results on the projected multi-layer network of plants are depicted in Fig. 12. Identifying clusters of plants with similar production capacities and good types through community clustering is vital for quickly adjusting production plans in response to demand fluctuations. This approach helps mitigating capacity imbalances across individual plants. If a plant halts production due to unforeseen circumstances, other similar plants can seamlessly take over its production tasks, ensuring supply chain continuity. Moreover, plants with similar production capacities and good types can rapidly switch between production lines to meet diverse good demands. This agile production strategy significantly reduces order fulfillment times and strengthens supply chain resilience.

Using clustering outcomes, flexible production strategies can be developed, including on-demand manufacturing and rapid production line switches. Establishing a robust risk

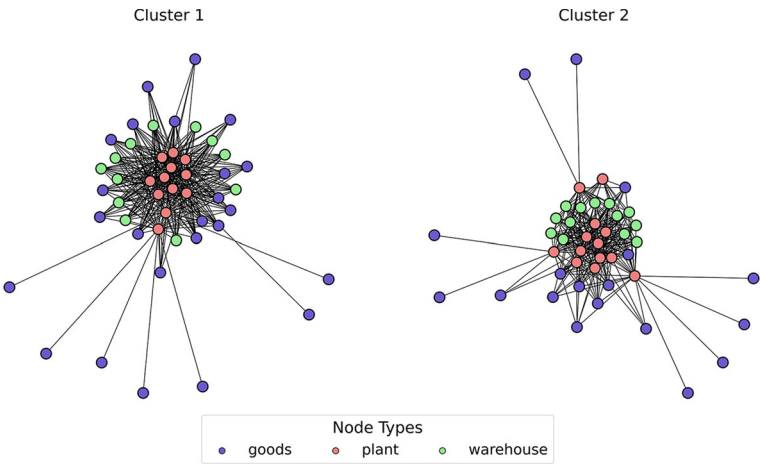

Fig. 13 2 clusters within the projected network of plants

alert and emergency response mechanism is equally crucial. For instance, during natural disasters or market fluctuations in specific regions, production and supply strategies can be quickly recalibrated to maintain supply chain stability. Figure 13, derived from community identification results, illustrates the connectivity features of Clusters 1 and 2. The edges represent various relationships connecting these plants, such as producing the same goods or collaborating with the same warehouses, implying similarities in production processes, resource allocation, and management operation models.

In Cluster 1, the interconnections among plants, goods, and warehouses are evenly distributed, resulting in a well-balanced network structure. This balance is evident in the allocation of resources, even distribution of node loads, and effective risk dispersion. Such an equilibrium enhances resource utilization, increases efficiency in the supply chain, and improves system resilience. Conversely, Cluster 2 exhibits significant imbalances in its network structure. Plant nodes experience uneven loads, leading to an unbalanced distribution of goods and warehouse nodes. Most goods nodes are clustered on one side of the network, while warehouse nodes are concentrated on the other, failing to distribute evenly across all plant nodes. This imbalance can create inefficiencies in resource utilization and compromise the overall stability and resilience of the supply chain.

Table 5 shows the network density and clustering coefficient for the goods and warehouse layers in both communities after clustering. Following community detection, the nodes within these clusters in both layers become fully connected. The network density of the goods layer increased from 0.483 to 1.000. This indicates that plants within a cluster likely share similar good types and production processes, promoting collaboration in addressing common challenges and opportunities. Additionally, plants within a cluster can form a mutual support network, enabling rapid assistance from other plants during times of difficulty or increased demand. This collective support bolsters the stability and resilience of the plants within the cluster.

(1) Flexibility Analysis of plants

Insufficient flexibility within the supply chain can significantly hinder a plant's ability to effectively respond to unforeseen events, such as disruptions in raw material supply or sudden surges in demand. Plants that produce a wide variety of goods can quickly adjust their

Table 5 Descriptive information of 2 clusters of plants

Network density			
Good layer	0.483	Warehouse layer	1.000
Cluster 1 (Good layer)	1.000	Cluster 1 (Warehouse layer)	1.000
Cluster 2 (Good layer)	1.000	Cluster 2 (Warehouse layer)	1.000
Clustering coefficient			
Plant layer	0.625	Warehouse layer	0.959
Cluster 1 (Plant layer)	0.759	Cluster 1 (Warehouse layer)	1.000
Cluster 2 (Plant layer)	0.516	Cluster 2 (Warehouse layer)	1.000

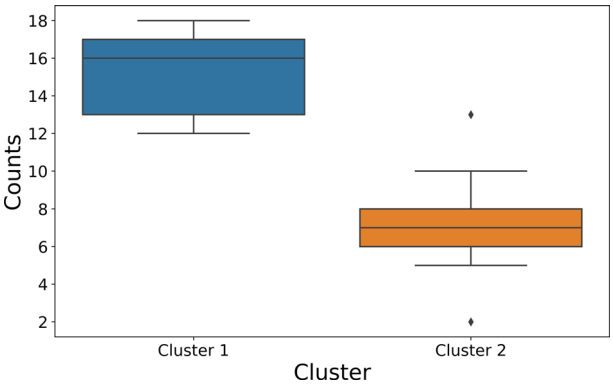

Fig. 14 The number of goods associated with plants for different clusters

production lines to meet changing market demands, thereby enhancing the supply chain's responsiveness and adaptability. Additionally, collaborating with multiple warehouses further enhances logistical and storage flexibility. This strategic approach allows plants to choose different warehouses for storage and distribution based on demand fluctuations, ultimately optimizing supply chain efficiency. In conclusion, the more diverse the range of goods a plant can produce and the more warehouses it collaborates with, the greater the flexibility and overall efficiency of the supply chain. Analyzing descriptive statistics and box plot comparisons of the number of goods produced by each plant, as shown in Fig. 14, reveals that plants in Cluster 1 produce approximately 16 goods. This indicates high production and storage flexibility.

Cluster 1 demonstrates the ability to quickly adjust production lines, adapt to market demand changes, and achieve on-demand production through flexible production lines. In contrast, plants in Cluster 2 produce a relatively limited range of goods, with the maximum good count in this cluster being close to the minimum in Cluster 1. This narrower range of production makes Cluster 2 plants less adaptable to market demand fluctuations. Their inability to rapidly shift to other goods may result in missed market opportunities and increased operational risks if market competition intensifies. Although fewer good types offer stability in production and management, they also constrain the overall flexibility of the supply chain. Cluster 2 plants may excel in specific product areas, but they are less capable of handling rapidly changing market environments. Over the long term, these plants could benefit from

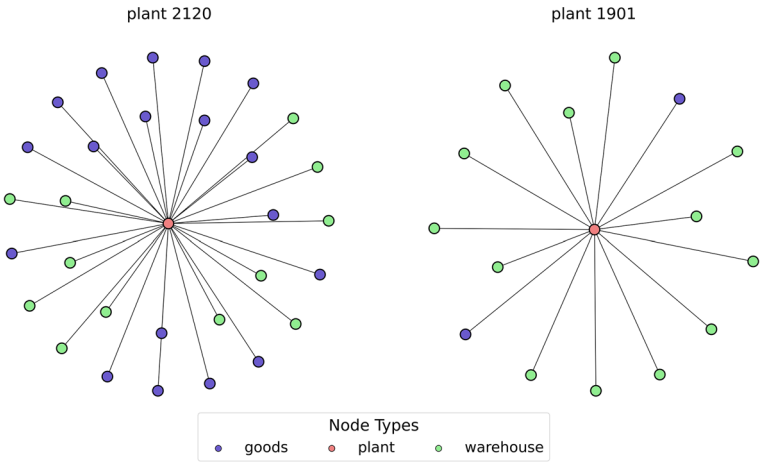

Fig. 15 Local networks of Node 2120 and Node 1901

gradually introducing new product lines, leveraging their existing production strengths and resources to enhance production diversity and supply chain flexibility.

Collaboration between plants in Cluster 1 and Cluster 2 with multiple warehouses helps mitigate storage risks and reduce the impact of single warehouse failures, such as those caused by natural disasters or fires. This strategy enhances the stability and reliability of the supply chain. Selecting one node from each community, as depicted in Fig. 15, visually confirms the flexibility analysis. The production flexibility of the plant node in Cluster 1 is nine times greater than that of the plant node in Cluster 2, while their storage flexibility remains almost identical.

(2) Redundancy Analysis of plants

A high similarity in the structure of goods produced by different plants indicates significant interchangeability in production lines, equipment, and processes. This interchangeability allows other plants to easily take over the production tasks of a disrupted plant, swiftly filling production gaps and ensuring the continuity of the supply chain. If a plant or warehouse becomes inoperable due to unforeseen circumstances, other highly similar plants or warehouses can quickly assume their functions, thereby mitigating the risk of supply chain disruptions. This risk mitigation mechanism enhances the stability and reliability of the supply chain.

The Jaccard coefficient is used to measure the correlation level between plants, indirectly assessing each plant's substitutability and determining the redundancy between the two clusters. The comparative results are presented in Fig. 16.

Within the same community, the Jaccard coefficient for each plant combination in the warehouse layer is uniformly 1. However, in the goods layer, Cluster 1 exhibits significantly more concentrated values compared to Cluster 2. Notably, the minimum Jaccard coefficient in Cluster 1 is higher than the median of Cluster 2. This indicates that Cluster 1 demonstrates strong redundancy due to high consistency in both cooperative warehousing and goods production. Any production or inventory issues in a plant within Cluster 1 can be quickly addressed by other plants. In contrast, although Cluster 2 maintains a high level of consistency in cooperative warehousing, it shows greater variability in goods production, resulting in weaker redundancy. Plants within Cluster 2 cannot fully substitute each other's production

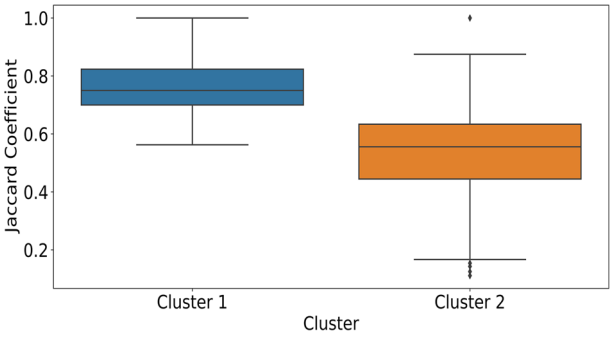

Fig. 16 Jaccard coefficients for plant combinations in goods

tasks. To enhance redundancy in Cluster 2, managers should implement centralized production planning and scheduling systems to achieve unified coordination of production tasks across plants.

Acknowledgements This research was funded by the Major Project of National Social Science Foundation of China (No. 22&ZD072), the National Natural Science Foundation of China (No. 72301070), Taiwan National Science Technology Coouncil (NSTC 112-2221- E-030-009-MY3).

Declarations

Conflict of interest The authors declare that they have no conflict of interest.

Open Access This article is licensed under a Creative Commons Attribution-NonCommercial-NoDerivatives 4.0 International License, which permits any non-commercial use, sharing, distribution and reproduction in any medium or format, as long as you give appropriate credit to the original author(s) and the source, provide a link to the Creative Commons licence, and indicate if you modified the licensed material. You do not have permission under this licence to share adapted material derived from this article or parts of it. The images or other third party material in this article are included in the article's Creative Commons licence, unless indicated otherwise in a credit line to the material. If material is not included in the article's Creative Commons licence and your intended use is not permitted by statutory regulation or exceeds the permitted use, you will need to obtain permission directly from the copyright holder. To view a copy of this licence, visit http://creativecommons.org/licenses/by-nc-nd/4.0/.

References

Chen, J., Sohal, A. S., & Prajogo, D. I. (2013). Supply chain operational risk mitigation: A collaborative approach. *International Journal of Production Research, 51*(7), 2186–2199.

Davoudi, S., Brooks, E., & Mehmood, A. (2013). Evolutionary resilience and strategies for climate adaptation. *Planning Practice & Research, 28*(3), 307–322.

Ellram, L. M., Tate, W. L., & Billington, C. (2004). Understanding and managing the services supply chain. *Journal of Supply Chain Management, 40*(3), 17–32.

Fan, Y., & Stevenson, M. (2018). A review of supply chain risk management: Definition, theory, and research agenda. *International Journal of Physical Distribution & Logistics Management, 48*(3), 205–230.

Gao, J., Barzel, B., & Barabási, A.-L. (2016). Universal resilience patterns in complex networks. *Nature, 530*(7590), 307–312.

Hendricks, K. B., & Singhal, V. R. (2003). The effect of supply chain glitches on shareholder wealth. *Journal of Operations Management, 21*(5), 501–522.

Ho, W., Zheng, T., Yildiz, H., & Talluri, S. (2015). Supply chain risk management: A literature review. *International Journal of Production Research, 53*(16), 5031–5069.

Huang, X., Chen, D., Ren, T., & Wang, D. (2021). A survey of community detection methods in multilayer networks. *Data Mining and Knowledge Discovery, 35*, 1–45.
Johnson, N., Elliott, D., & Drake, P. (2013). Exploring the role of social capital in facilitating supply chain resilience. *Supply Chain Management: An International Journal, 18*(3), 324–336.
Jüttner, U., Peck, H., & Christopher, M. (2003). Supply chain risk management: Outlining an agenda for future research. *International Journal of Logistics: Research and Applications, 6*(4), 197–210.
Kim, J., & Lee, J.-G. (2015). Community detection in multi-layer graphs: A survey. *ACM SIGMOD Record, 44*(3), 37–48.
Kristianto, Y., Gunasekaran, A., Helo, P., & Hao, Y. (2014). A model of resilient supply chain network design: A two-stage programming with fuzzy shortest path. *Expert Systems with Applications, 41*(1), 39–49.
Lei, J., Chen, K., & Lynch, B. (2019). Consistent community detection in multi-layer network data. *Biometrika, 107*(1), 61–73.
Ma, X., Dong, D., & Wang, Q. (2018). Community detection in multi-layer networks using joint nonnegative matrix factorization. *IEEE Transactions on Knowledge and Data Engineering, 31*(2), 273–286.
Ma, Z., & Nandy, S. (2023). Community detection with contextual multilayer networks. *IEEE Transactions on Information Theory, 69*(5), 3203–3239.
Maharjan, R., & Kato, H. (2022). Resilient supply chain network design: A systematic literature review. *Transport Reviews, 42*(6), 739–761.
Mandal, S. (2012). An empirical investigation into supply chain resilience. *IUP Journal of Supply Chain Management, 9*(4).
Mentzer, J. T., DeWitt, W., Keebler, J. S., Min, S., Nix, N. W., Smith, C. D., & Zacharia, Z. G. (2001). Defining supply chain management. *Journal of Business Logistics, 22*(2), 1–25.
Norrman, A., & Wieland, A. (2020). The development of supply chain risk management over time: Revisiting Ericsson. *International Journal of Physical Distribution & Logistics Management, 50*(6), 641–666.
Pavlov, A., Ivanov, D., Pavlov, D., Slinko, A.: Optimization of network redundancy and contingency planning in sustainable and resilient supply chain resource management under conditions of structural dynamics. *Annals of Operations Research,* 1–30 (2019).
Sodhi, M. S., Son, B.-G., & Tang, C. S. (2012). Researchers' perspectives on supply chain risk management. *Production and Operations Management, 21*(1), 1–13.
Son, B.-G., Chae, S., & Kocabasoglu-Hillmer, C. (2021). Catastrophic supply chain disruptions and supply network changes: A study of the 2011 Japanese earthquake. *International Journal of Operations & Production Management, 41*(6), 781–804.
Tagarelli, A., Amelio, A., & Gullo, F. (2017). Ensemble-based community detection in multilayer networks. *Data Mining and Knowledge Discovery, 31*, 1506–1543.
Tukamuhabwa, B. R., Stevenson, M., Busby, J., & Zorzini, M. (2015). Supply chain resilience: Definition, review and theoretical foundations for further study. *International Journal of Production Research, 53*(18), 5592–5623.
Wasi, A. T., Islam, M. S., Akib, A. R. (2023). Supplygraph: A benchmark dataset for supply chain planning using graph neural networks. In *4th Workshop on graphs and more complex structures for learning and reasoning, 38th annual AAAI conference on artificial intelligence*.
Wieland, A., & Durach, C. F. (2021). *Two perspectives on supply chain resilience*. Wiley Online Library.

Publisher's Note Springer Nature remains neutral with regard to jurisdictional claims in published maps and institutional affiliations.